Earth Planet. Sci. Lett. 696 (2026) 120409

Contents lists available at ScienceDirect

Earth and Planetary Science Letters

journal homepage: www.elsevier.com/locate/epsl

Hot Archean orogens suppressed voluminous S-type granite formation

Ming Tang [a,*], Zi Ye [a], Xu Chu [b]

[a] SKLab-DeepMinE, MOEKLab-OBCE, School of Earth and Space Sciences, Peking University, China
[b] Department of Earth Sciences, University of Toronto, 22 Ursula Franklin Street, Toronto, Ontario, M5S 3B1, Canada

ARTICLE INFO

Editor: Dr Fang-Zhen Teng

Keywords:
Early earth
S-type granites
Crustal thermal state
Decompression melting
Exhumation
Continent formation

ABSTRACT

S-type granites are far less abundant during much of the Archean than in the Phanerozoic, and this paucity remains puzzling. We propose that the suppression of S-type granite formation at scale may have been an inherent consequence of the hotter Archean crust. A key insight from fossil P-T-t paths in representative orogens is that the onset of melting can trigger exhumation and thereby limit the maximum burial depth of sediments. In a hot crust, this maximum burial depth is relatively shallow, because hot geotherms initiate melting at shallow depths due to the pressure dependence of dehydration melting. By contrast, colder geotherms in Phanerozoic orogens effectively suppress melting until higher pressures and temperatures. As a result, Archean sedimentary packages were exhumed too early to undergo extensive decompression and dehydration melting attainable in modern cycles. Phase equilibria modeling shows that the exhuming metasediments in the Archean may only generate melt fractions 1/3 to 1/2 of those in the Phanerozoic. Such low melt productivity in the Archean may have inhibited the formation of large S-type plutons and batholiths. More broadly, these processes may have impeded deep recycling of sediments and, by limiting upward distillation of heat-producing elements, slowed the cooling of the Archean continental crust.

1. Introduction

Earth evolves through continuous interactions between its surface processes and deep-seated tectonic cycles (Cawood et al., 2022). Weathering and erosion transform continental crust into clastic sediments, which may later be buried deep within the lithosphere during mountain building events. At depth, these metamorphosed sediments eventually melt to form S-type granites—peraluminous to strongly peraluminous granites that record the coupled evolution of Earth's surface environment and its long-term tectonic history (Chappell and White, 1992; Frost and Da Prat, 2021).

S-type granites are rare in rock records on early Earth. Preserved Archean crusts are dominated by TTGs (tonalite–trondhjemite–granodiorite) interpreted to have formed from basalt remelting (Johnson et al., 2019; Moyen and Martin, 2012). The oldest S-type granites with strongly peraluminous compositions are Mesoarchean in age, and occur as small intrusions (Barton et al., 1987; Bucholz and Spencer, 2019; Poujol et al., 2021). Later in the Neoarchean, S-type granites became more widespread (Breaks and Moore, 1992; Bucholz, 2025; Poujol et al., 2021). It is also possible to track the occurrence of S-type granite magmatism from detrital zircons, although this approach heavily relies on zircon provenance proxies. A recent machine learning study (Jiang et al., 2024) indicates voluminous S-type granites present in Earth's crust since the Hadean. The robustness of Jiang et al.'s zircon classification model can be further tested using additional training and data, particularly from Archean S-type granites. By contrast, all other zircon proxy-based studies imply limited S-type granite magmatism in the Hadean and Archean (Burnham and Berry, 2017; Roberts et al., 2024; Trail et al., 2017; Zhu et al., 2020).

Several hypotheses may provide insights into the paucity of S-type granites on early Earth. One possibility is that extensive subaerial crust did not emerge until the Neoarchean (Bindeman et al., 2018; Chowdhury et al., 2025), limiting the production of clastic sediments (Frost and Da Prat, 2021; Zhu et al., 2020). However, abundant clastic sedimentary successions have been documented in many Archean cratons, and many of them were deposited in the Mesoarchean or earlier (Supplementary Material 3). Examples include the 3.4 Ga Strelley Pool Formation in the Pilbara Craton (Hickman, 2023), the 3.2 Ga Moodies Group and 3.0–2.8 Ga Witwatersrand-Pongola Supergroup in the Kaapvaal Craton (Kröner and Hofmann, 2019), and the ~2.9 Ga Central Slave Cover Group in the Slave Craton (Bleeker et al., 1999). These ancient successions suggest that Earth's surface was not devoid of clastic

* Corresponding auther.
E-mail address: mingtang@pku.edu.cn (M. Tang).

https://doi.org/10.1016/j.epsl.2026.120409
Received 12 May 2026; Received in revised form 26 September 2026; Accepted 9 October 2026
0012-821X/© 2026 Elsevier B.V. All rights are reserved, including those for text and data mining, AI training, and similar technologies.

sediments since the Paleoarchean, although the emergence of subaerial crust may have been intermittent in the early Archean.

Alternatively, plate tectonics may not have been fully operative through most of the Archean (Cawood et al., 2022; Dhuime et al., 2012; Tang et al., 2016) so that sediments cannot be buried by plate convergence. A key challenge for this hypothesis is that exactly when plate tectonics started remains highly uncertain (Arndt, 2013; Palin et al., 2020). Moreover, It remains unclear whether plate tectonics is the sole tectonic regime capable of transporting sediments to Earth's interior (Chelle-Michou et al., 2022). In any case, a number of observations have shown that deep recycling of crustal rocks that had interacted with seawater and atmosphere was possible in the Archean (Deng et al., 2019; Ge et al., 2023; Tamblyn et al., 2023; Wang et al., 2022).

Preservation bias may introduce additional complexities, but it is unlikely to fully explain the scarcity of Archean S-type granites relative to TTGs. First, TTGs and S-type granites have broadly similar chemical and mineralogical compositions, and thus similar weathering susceptibilities. Even if S-type granites were preferentially removed by erosion, the detrital zircon records do not support more abundant S-type granites except for the results of Jiang et al. (2024).

While the mechanisms outlined above remain possible, they critically depend on key assumptions that are difficult to test with current observations. Here, we take a different approach and address whether and why S-type granites may have been rare in the Archean from a tectonic-magmatic coupling perspective.

2. Exhumation, decompression melting, and S-type granite formation

One clear clue is that S-type granites predominantly form during orogenic collapse (Collins and Richards, 2008; Sylvester, 1998). Clastic sediments deposited at the surface are buried into the deep crust during orogenic compression and crustal thickening. At this burial stage, however, sediment melting is limited because thermal lag delays heating and the sediments typically follow a shallow T/P path during burial (Philpotts and Ague, 2022). Orogenic collapse subsequently causes crustal thinning and exhumation of deep buried metasediments. During exhumation, pressure drops rapidly, but thermal lag slows cooling as deep, hot metasediments rise. Additional heat supplied by mantle upwelling, where present, may cause the rising metasediments to follow a near-isothermal decompression path with or without thermal relaxation (Ji et al., 2024; Whitney et al., 2004). Because anatexis is largely controlled by pressure-dependent muscovite and biotite dehydration melting (Thompson, 1982; White et al., 2007), this decompression as well as slow cooling may lead to extensive melting. Therefore, the formation of S-type granite at scale reflects the combined effects of thermal lag during both burial and exhumation, and the pressure dependence of metasediment dehydration melting (Fig. 1).

3. Melting-limited burial of sediments

Of particular interest here is the initiation of exhumation, which determines both the maximum burial depth and the extent of subsequent decompression melting. There is no doubt that exhumation at scale is often driven by tectonic processes, but regardless of the tectonic context, melting can also initiate exhumation, and this process limits how deep sediments can be buried in orogenic crust. Once melting occurs, the bulk density of the metasedimentary package decreases, and buoyancy drives upward migration of the package (Mintrone et al., 2022; Vanderhaeghe, 2009). More importantly, a small fraction of melt (5–7%) can dramatically reduce the strength of rocks (Rosenberg and Handy, 2005) and result in strain localization (Brown, 2001; Hollister, 1993). As a consequence, further burial is largely terminated, and exhumation may then take place either along melt-lubricated shear zones or by diapiric ascent (Hollister and Crawford, 1986; Whitney et al., 2004).

Metamorphic records from many orogenic terranes support melting-limited burial (Fig. 2). Based on the classification of Brown and Johnson (2018), we compiled clockwise P-T-t paths of metasediments in intermediate and high T/P series, which reflect burial and exhumation during mountain building and collapse. Prograde paths are typically poorly constrained, and peak pressures are partially overprinted by low-pressure, high-temperature metamorphism during exhumation (Groppo et al., 2007). Despite these uncertainties, the initiation of exhumation, inferred from the peak pressures along these paths, plot within or close to the nascent melting regime of average shales (Fig. 2). These observations are consistent with the suggestion that the onset of melting can initiate exhumation and thus set an upper bound on the depth of sediment burial.

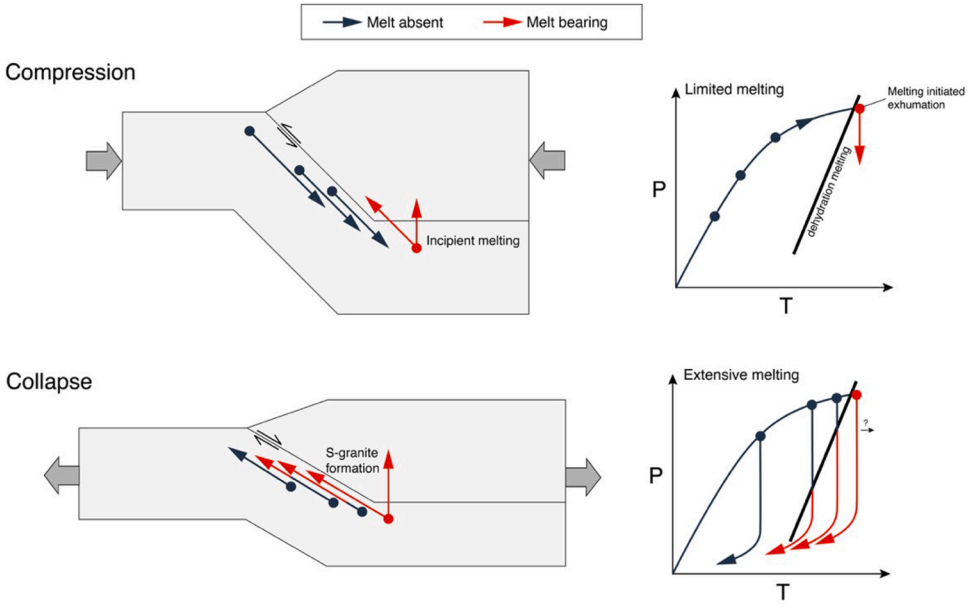


Fig. 1. Conceptual diagram showing burial, exhumation, and decompression-driven melting of metasediments in an orogenic cycle. Because of thermal lag, melting is more extensive during exhumation, which takes place at scale during orogen collapse.

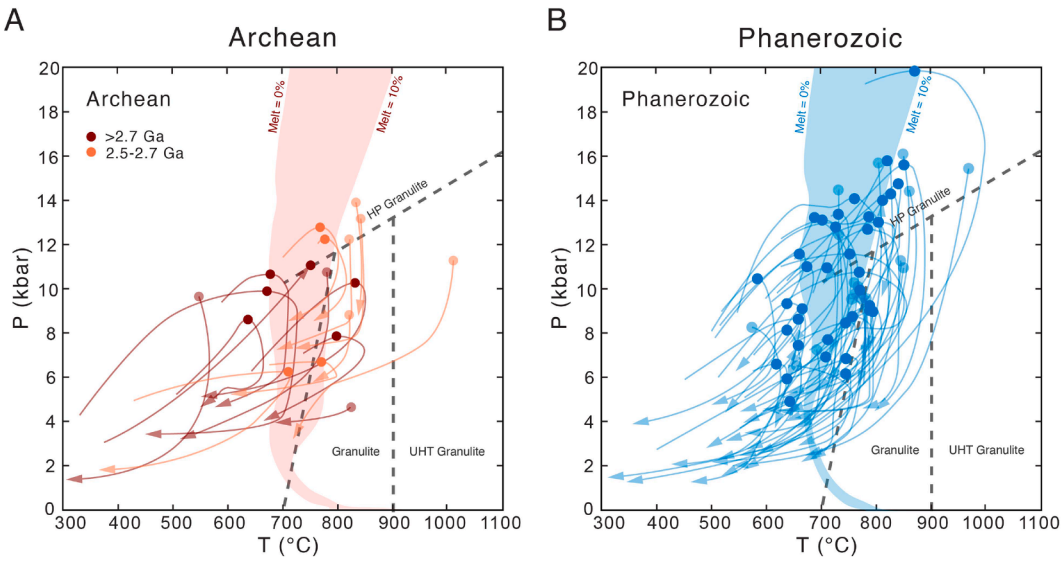


Fig. 2. Clockwise P-T-t paths of sediment metamorphism in the Archean and Phanerozoic. Archean paths are subdivided into pre-2.7 Ga and 2.7–2.5 Ga groups since strongly peraluminous granites became more prominent near the end of the Archean. Filled circles mark the inferred burial-to-exhumation transitions. For paths lacking a discernible prograde segment, the corresponding transition is shown with a faded symbol. The red and blue shaded areas mark the 0–10% melting windows of average Archean and Phanerozoic shales, respectively (Condie, 1993); they provide a reference for nascent melting conditions of clastic metasediment, although the exact melting conditions may vary with metasediment composition. Note that the Archean metasediments exhibit systematically lower pressures than their Phanerozoic counterparts. Sources of P-T-t paths are listed in the Supplementary Material 2.

4. Maximum melting potential linked to burial T/P gradient

Melt productivity, or melting potential, during subsequent decompression is strongly influenced by the pressure and temperature conditions at burial-exhumation transition. High initial pressure and temperature conditions allow rocks to undergo extensive decompression and yield greater melting potentials because metasediment dehydration melting is pressure-dependent (Fig. 3). This same pressure dependence makes the T/P gradient of the burial path critical, as it determines where the burial path passes the solidus. Given the melting-limited burial discussed above, the burial T/P gradient ultimately determines the maximum depth of the burial-exhumation transition. Along a hot (high T/P) burial path, metasediments pass solidus at relatively low pressure and temperature conditions and are exhumed early on. By contrast, along a cold (low T/P) path, metasediments can be buried to greater depth before melting occurs and triggers exhumation. Therefore, metasediments buried along a hot path are expected to produce systematically less melt during exhumation than those buried along a cold path. Although this conclusion may seem counterintuitive, it follows naturally from the coupling between melting and exhumation.

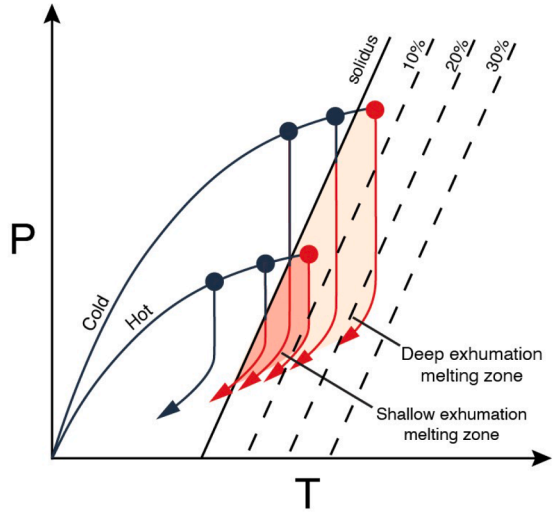


Fig. 3. Conceptual diagram showing the influence of burial T/P gradient on maximum melting potential during exhumation. For simplicity, this conceptual diagram illustrates the idea with a widely occurring scenario of isothermal decompression. Both cooling and heating are possible during decompression, but the systematic difference in melting potential for deep vs. shallow exhumation remains unchanged.

5. Archean hot crust reduced sediment melting potential

We now turn to the formation of S-type granites in the Archean. The Archean tectonic regime is highly uncertain, and sediment burial may have been driven by either Phanerozoic-style orogenesis or sagduction (see discussion below). Nevertheless, the crust in the Archean is widely thought to have been hotter than in the Phanerozoic (Condie, 1984) due to a hotter underlying mantle and greater radiogenic heat production (Herzberg et al., 2010; Lee and Chin, 2014). Accordingly, hotter Archean orogens would have promoted hotter burial and shallower exhumation. This inference is supported by the lack of high-pressure metamorphism in the Archean. Specifically, metasediments of high-pressure granulite facies were rare in the Archean (Fig. 2A), and the few known examples occurred near the end of the Archean (O'brien and Rötzler, 2003), including those in the North China Craton (Wang and Guo, 2017) and North Atlantic Craton (Dyck et al., 2015). This is also when S-type granites became more widespread in major Archean cratons (Bucholz, 2025). By contrast, high-pressure pelitic granulites became more widespread in the Phanerozoic (Fig. 2B).

We used phase equilibria modeling to estimate the maximum melting potential of metasediments during exhumation in the Archean and Phanerozoic orogens. We considered graywackes and shales (metapelites) as two endmember source rocks of S-type granites (Chappell and White, 1992). For simplicity, we modeled isothermal decompression from the pressure and temperature conditions at which 7% melting is reached. This isothermal decompression terminates in the middle to upper crust (~5 kbar), after which cooling takes place with slower exhumation. We adopted 7% melting as the critical point of burial-exhumation transition because the presence of 5–7% melts

dramatically reduces the strength of rocks (Rosenberg and Handy, 2005). Since not all sediments are buried to the depth of melting before exhumation initiates, our calculated melting potentials represent the upper bounds. These burial-exhumation paths are no doubt highly simplified, but they provide reasonable contexts for evaluating how contrasting crustal thermal regimes influenced sediment burial and melting in the Archean vs. Phanerozoic. We also note that Archean shales tend to have higher Mg and Fe contents than the Phanerozoic ones (Table S1), likely reflecting the more mafic composition in Archean crusts (Tang et al., 2016), and/or interactions with the ferruginous oceans (Swanner et al., 2020). This compositional difference further lowers melting potential of the Archean shales because higher bulk Mg and Fe contents favor biotite relative to muscovite.

Intermediate T/P series is interpreted to reflect Barrovian-type metamorphism typical of thickened orogenic crust (Brown and Johnson, 2018). If their average T/P are taken to approximate those of the burial paths (67 ± 7 °C/kbar vs. 55 ± 12 °C/kbar (1 σ) for the Archean and Phanerozoic, respectively), then both graywackes and shales can hardly be buried to > 14 kbar in the Archean but could reach up to 18–20 kbar in the Phanerozoic (Figs. 4 and 5). Because of this shallower burial, Archean metasediments undergo substantially lower degrees of melting during decompression. Shales are more fertile than graywackes in terms of melt production along the same burial-exhumation paths. For a graywacke-dominated source, decompression melting can reach 10–20% in the Phanerozoic but remains below 10% in the Archean (Fig. 4); for a shale-dominated source, melting can reach 30–50% in the Phanerozoic but terminates at 10–20% in the Archean (Fig. 5). We also modeled melting of 50% shales + 50% graywackes as these sedimentary lithologies are usually interbedded (Supplementary Material 3). The results are provided in Supplementary Material 1 and also show a pronounced contrast in melt production between the Archean and Phanerozoic. Overall, maximum melt fractions in Archean metasediments are roughly 1/3 - 1/2 of those of the Phanerozoic. Consequently, hot Archean orogens may have formed voluminous melt-bearing migmatites but supplied limited extractable melts to assemble voluminous S-type plutons (Fig. 6). This conclusion is

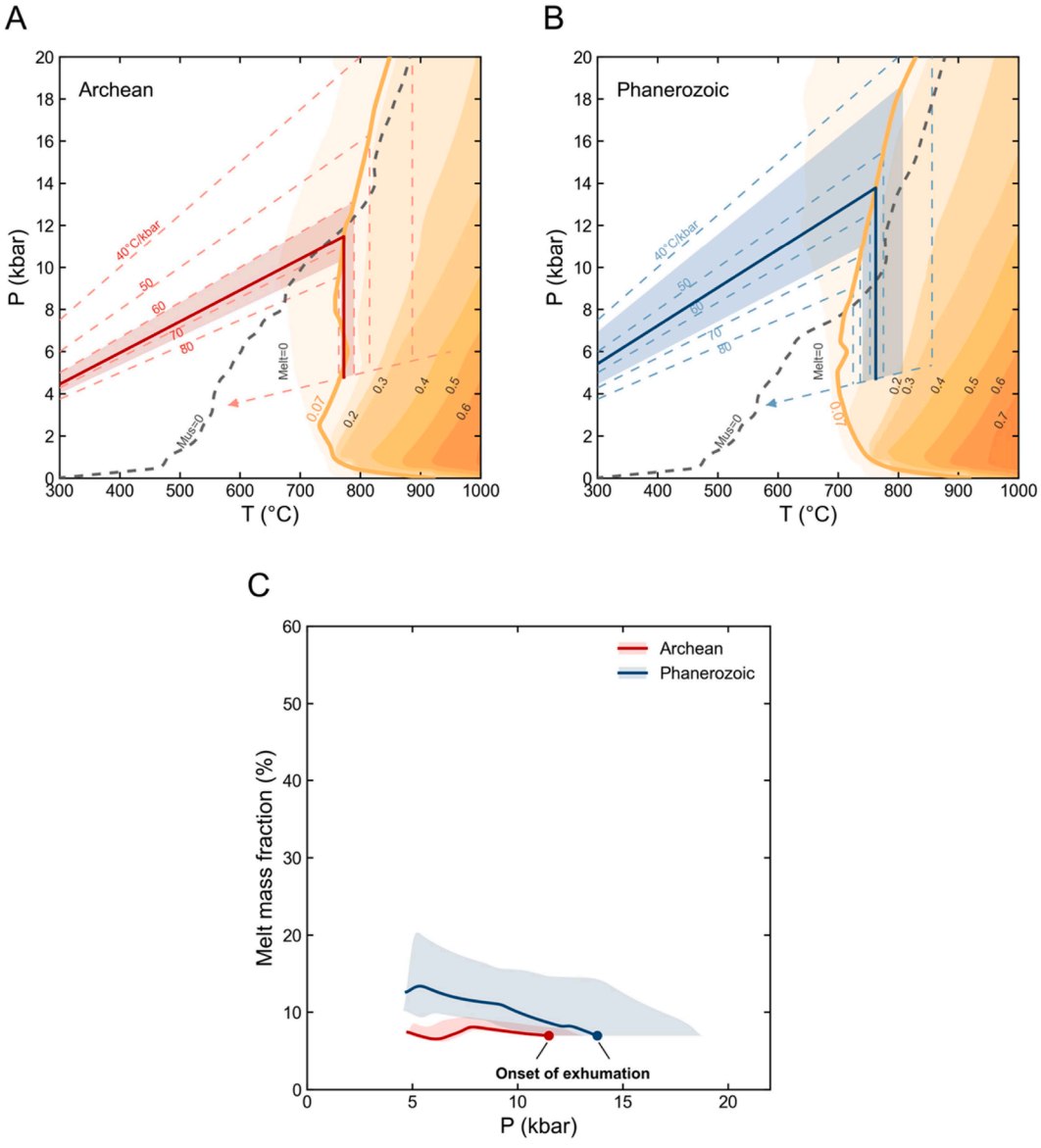


Fig. 4. Melting of graywackes in the Archean vs. Phanerozoic orogens. A and **B**. Burial-exhumation paths with various burial T/P gradients. These paths represent the maximum burial depth scenarios in which the burial-exhumation transitions are triggered by melting. See texts for explanation. The bold lines and shaded areas plot the paths along the mean T/P gradients of intermediate T/P metamorphism with 1 σ envelopes. The melt fraction contours are from phase equilibria modeling. **C.** Melt production along the exhumation paths shown in A and B.

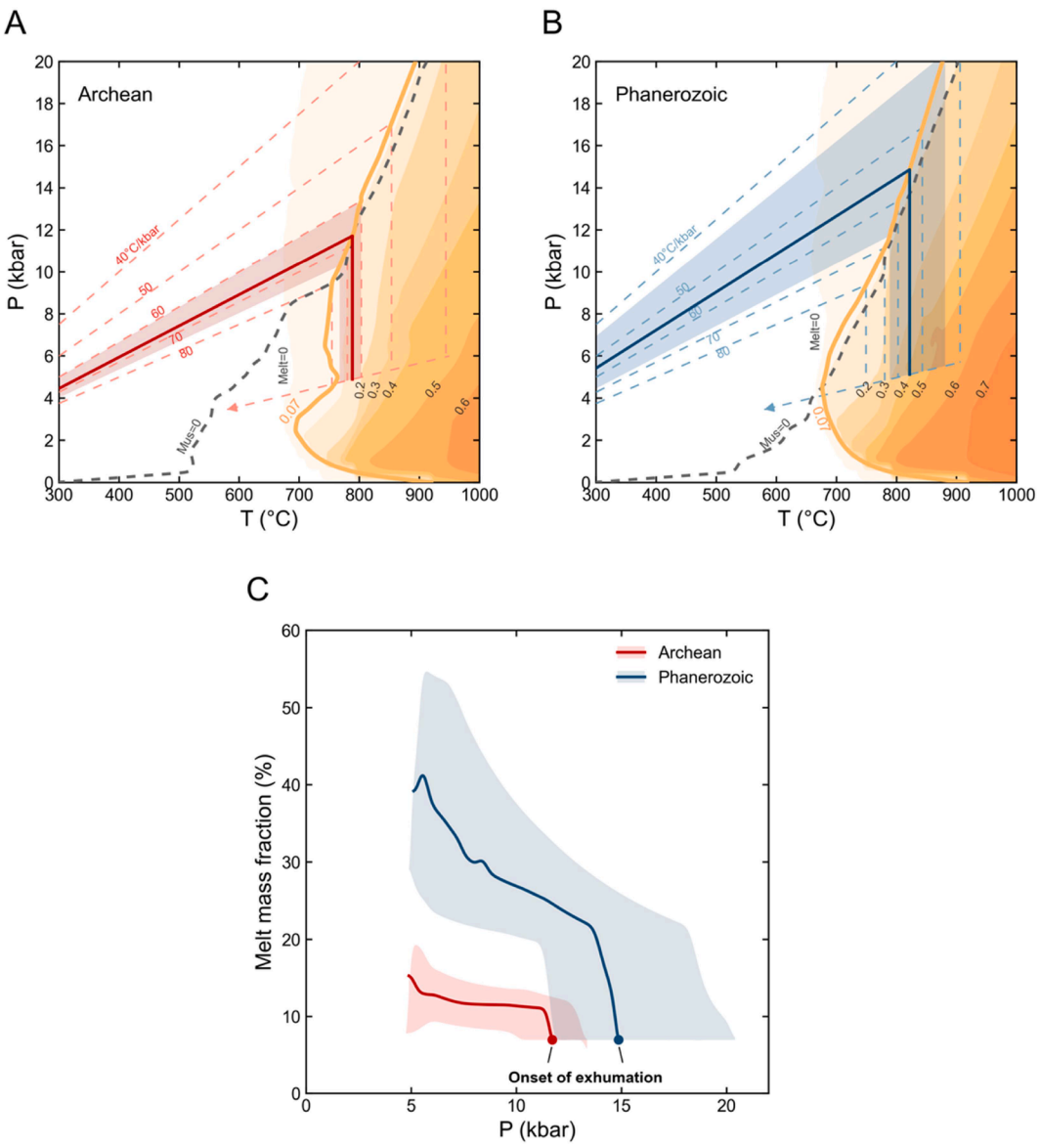


Fig. 5. Melting of shales (metapelites) in the Archean vs. Phanerozoic orogens. See Fig. 4 for more details of figure explanation.

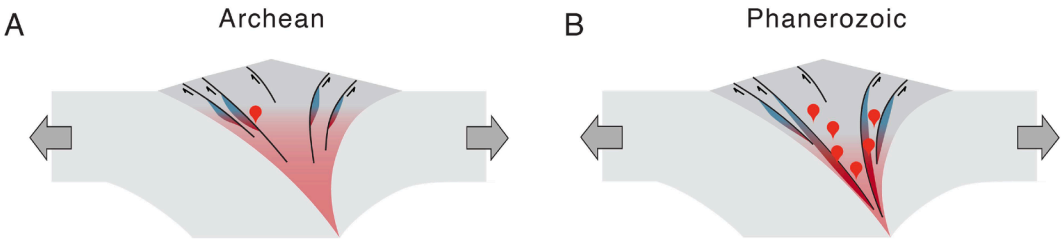


Fig. 6. Cartoon illustrating exhumation and melting of buried sediments in the Archean vs. Phanerozoic. Owing to melting-limited burial, sediments can only be buried to shallow depth in the hot Archean crust before exhumation initiates. This shallow burial reduced the decompression melting potential during subsequent exhumation.

consistent with the widespread occurrence of paragneissic migmatites in most major Archean cratons (Block et al., 2013; Donohue and Essene, 2005; Dziggel et al., 2014; Guevara et al., 2017; Millonig et al., 2008; Nicoli et al., 2015; Taylor et al., 2012; Valli et al., 2004; Wang and Guo, 2017).

6. Complexities and caveats

While the average burial T/P gradients imply limited deep burial and melting of sediments in the Archean, our model does not preclude the possibility of localized deep burial in certain tectonic settings. For instance, small sedimentary bodies may be encapsulated within other units and transported to greater depths. In addition, substantial

radiogenic heat production within the crust may also cause significant heating and thereby enhance melting (Clark et al., 2011). Such cases have been documented in both the Archean and Phanerozoic metamorphic records (Fig. 2). However, these processes do not, on a first order, negate the systematic contrast in maximum burial pressure and melt productivity between the hot Archean and cold Phanerozoic crust.

Another complexity arises if sediment burial and exhumation in the Archean were dominated by sagduction, which likely formed the dome-and-keel structures seen in many Archean cratons (Macgregor, 1951). Metamorphic P-T-t paths associated with sagduction are not necessarily clockwise as assumed here (Yu et al., 2022; Zhao and Zhai, 2013). In the case of counterclockwise P-T-t paths, burial in response to magmatic loading would take place along even hotter T/P gradients, and exhumation/decompression may lag behind cooling (Zhao and Zhai, 2013). Both effects could further hinder decompression melting and thus reduce melt productivity.

Our findings emphasize exhumation and decompression melting in S-type granite formation, but this mechanism need not be the dominant explanation for the paucity of S-type granites in the Archean. Limited continental emergence (Chowdhury et al., 2025) may have restricted the supply of clastic sediments in the Archean. While sediment availability determines whether the source rocks of S-type granites existed, our exploration addresses whether these sediments, if present, could produce enough melt to form large S-type plutons.

7. Conclusions and implications

Our conceptual model underscores a fundamental control of crustal thermal conditions on sediment burial and melting. Critical to our model is melting-limited burial of sediments, wherein the onset of melting triggers exhumation, and thereby caps the maximum burial depth. This mechanism is based on the physical responses of rocks to melting, including density reduction and mechanical weakening. Melting-limited burial should thus operate irrespective of the tectonic process driving burial, be it horizontal compression or vertical sagduction. Consequently, hotter Archean crust would have inherently suppressed S-type granite generation at scale, regardless of the debated tectonic regime in the Archean.

Two important implications may follow. First, shallow initiation of exhumation may have largely confined clastic sediment recycling to the upper ~40 km of the lithosphere on early Earth. This may partially explain the lack of K-rich calc-alkaline rocks until the Neoarchean. K-rich calc-alkaline rocks are widespread in Phanerozoic magmatic orogens, and their high K contents may result from clastic sediment incorporation in the sources (Gao et al., 2026; Plank and Langmuir, 1993). Although the scarcity of clastic sediments in the Archean remains possible, hindered recycling of these sediments may have further diminished their influence on deep crustal or mantle magmatism.

Another important consequence pertains to crustal thermal evolution and differentiation. Clastic sediments are enriched in heat-producing elements (K, Th, and U) (Hasterok et al., 2018). Clastic sediment burial thus increases heat production of the crustal interior and heats the crust. Partial melting of these buried sediments can facilitate crustal cooling by extracting heat-producing elements into melts which then rise, solidify, and are ultimately eroded away. This melting-driven upward distillation and erosional stripping of heat-producing elements are critical to cooling and stabilization of the continental crust (Reimink and Smye, 2024; Smye and Kelemen, 2025). However, our work suggests that extensive melting of metasediments may have been inherently suppressed in the hot Archean crust due to shallow burial. As a result, a large proportion of the heat-producing elements remain locked up in the crust containing bodies of metasedimentary rocks that underwent limited melting. Therefore, other mechanisms must have been operating to cool the crust before deep burial and extensive decompression melting became more efficient. In this context, widespread segregation of peraluminous melts and emplacement of S-type granites in the Neoarchean marks either the completion of cratonization or substantial cooling of the ambient mantle.

CRediT authorship contribution statement

Ming Tang: Writing – original draft, Methodology, Investigation, Funding acquisition, Formal analysis, Conceptualization. **Zi Ye:** Writing – review & editing, Methodology, Formal analysis. **Xu Chu:** Writing – review & editing, Validation.

Declaration of competing interest

The authors declare that they have no known competing financial interests or personal relationships that could have appeared to influence the work reported in this paper.

Acknowledgements

We thank Chris Hawkesworth and an anonymous reviewer for their constructive and thoughtful comments. This work was financially supported by the National Natural Science Foundation of China and the Ministry of Science and Technology of China (grants 42125302 and 2023YFF0803801). M.T. is grateful for the support from the Xplorer Prize.

Supplementary materials

Supplementary material associated with this article can be found, in the online version, at doi:10.1016/j.epsl.2026.120409.

Data availability

Available in the Supplementary Materials.

References

Arndt, N.T., 2013. Formation and evolution of the continental crust. Geochem. Perspect. 2, 405–533.
Barton, J.M., Klemd, R., Allsopp, H.L., Auret, S.H., Copperthwaite, Y.E., 1987. The geology and geochronology of the Annandagstoppane granite, Western Dronning Maud Land, Antarctica. Contrib. Mineral. Petrol. 97, 488–496.
Bindeman, I.N., Zakharov, D.O., Palandri, J., Greber, N.D., Dauphas, N., Retallack, G.J., Hofmann, A., Lackey, J.S., Bekker, A., 2018. Rapid emergence of subaerial landmasses and onset of a modern hydrologic cycle 2.5 billion years ago. Nature 557, 545–548.
Bleeker, W., Ketchum, J.W., Jackson, V.A., Villeneuve, M.E., 1999. The Central Slave Basement Complex, Part I: its structural topology and autochthonous cover. Can. J. Earth. Sci. 36, 1083–1109.
Block, S., Moyen, J.-F., Zeh, A., Poujol, M., Jaguin, J., Paquette, J.-L., 2013. The Murchison Greenstone Belt, South Africa: accreted slivers with contrasting metamorphic conditions. Precambrian. Res. 227, 77–98.
Breaks, F.W., Moore, J.M., 1992. The Ghost Lake Batholith, Superior Province of northwestern Ontario; a fertile, S-type, peraluminous granite-rare-element pegmatite system. Can. Mineral. 30, 835–875.
Brown, M., 2001. Orogeny, migmatites and leucogranites: a review. J. Earth Syst. Sci. 110, 313–336.
Brown, M., Johnson, T., 2018. Secular change in metamorphism and the onset of global plate tectonics. Am. Mineral. 103, 181–196.
Bucholz, C.E., 2025. The diversity and origin of granites. In: Anbar, A., Weis, D. (Eds.), Treatise on Geochemistry, 3rd edition. Elsevier, Oxford, pp. 153–202.
Bucholz, C.E., Spencer, C.J., 2019. Strongly peraluminous granites across the archean–Proterozoic transition. J. Petrol. 60, 1299–1348.
Burnham, A.D., Berry, A.J., 2017. Formation of Hadean granites by melting of igneous crust. Nat. Geosci. 10, 457–461.
Cawood, P.A., Chowdhury, P., Mulder, J.A., Hawkesworth, C.J., Capitanio, F.A., Gunawardana, P.M., Nebel, O., 2022. Secular evolution of continents and the Earth System. Rev. Geophys. 60, e2022RG000789.
Chappell, B.W., White, A., 1992. I-and S-type granites in the Lachlan Fold Belt. Earth Environ. Sci. Trans. R. Soc. Edinb. 83, 1–26.
Chelle-Michou, C., McCarthy, A., Moyen, J.-F., Cawood, P.A., Capitanio, F.A., 2022. Make subductions diverse again. Earth-Sci. Rev. 226, 103966.
Chowdhury, P., Cawood, P.A., Mulder, J.A., 2025. Subaerial emergence of continents on archean Earth. Annu. Rev. Earth Planet. Sci. 53, 443–478.
Clark, C., Fitzsimons, I.C., Healy, D., Harley, S.L., 2011. How does the continental crust get really hot? Elements 7, 235–240.

Collins, W., Richards, S., 2008. Geodynamic significance of S-type granites in circum-pacific orogens. Geology 36, 559.
Condie, K.C., 1984. Archean geotherms and supracrustal assemblages. Tectonophysics 105, 29–41.
Condie, K.C., 1993. Chemical composition and evolution of the upper continental crust: contrasting results from surface samples and shales. Chem. Geol. 104, 1–37.
Deng, Z., Chaussidon, M., Guitreau, M., Puchtel, I.S., Dauphas, N., Moynier, F., 2019. An oceanic subduction origin for Archaean granitoids revealed by silicon isotopes. Nat. Geosci. 12, 774–778.
Dhuime, B., Hawkesworth, C.J., Cawood, P.A., Storey, C.D., 2012. A change in the geodynamics of continental growth 3 billion years ago. Science 335, 1334–1336.
Donohue, C.L., Essene, E.J., 2005. Granulite-facies conditions preserved in vanadium- and chromium-rich metapelites from the Paradise Basin, Wind River Range, Wyoming, USA. Can. Mineral. 43, 495–511.
Dyck, B., Reno, B.L., Kokfelt, T.F., 2015. The Majorqaq Belt: a record of neoarchaean orogenesis during final assembly of the North Atlantic Craton, southern West Greenland. Lithos 220-223, 253–271.
Dziggel, A., Diener, J., Kolb, J., Kokfelt, T., 2014. Metamorphic record of accretionary processes during the neoarchaean: the Nuuk region, southern West Greenland. Precambrian. Res. 242, 22–38.
Frost, C.D., Da Prat, F.A., 2021. Petrogenetic and tectonic interpretation of strongly peraluminous granitic rocks and their significance in the Archean rock record. Am. Mineral. 106, 1195–1208.
Gao, M., Wang, Y., Xu, Y.-G., 2026. Progressive sub-arc mantle oxidation modulated by sediment melt. Sci. Adv. 12, eaeb9023.
Ge, R.-F., Wilde, S.A., Zhu, W.-B., Wang, X.-L., 2023. Earth's early continental crust formed from wet and oxidizing arc magmas. Nature 623, 334–339.
Groppo, C., Lombardo, B., Rolfo, F., Pertusati, P., 2007. Clockwise exhumation path of granulitized eclogites from the Ama Drime range (Eastern Himalayas). J. Metamorph. Geol. 25, 51–75.
Guevara, V.E., Caddick, M.J., Dragovic, B., 2017. Rapid high-T decompression recorded by Archean granulites in the northern Wyoming Province: insights from petrological modelling. J. Metamorph. Geol. 35, 943–965.
Hasterok, D., Gard, M., Webb, J., 2018. On the radiogenic heat production of metamorphic, igneous, and sedimentary rocks. Geosci. Front. 9, 1777–1794.
Herzberg, C., Condie, K., Korenaga, J., 2010. Thermal history of the Earth and its petrological expression. Earth. Planet. Sci. Lett. 292, 79–88.
Hickman, A.H., 2023. Archean Evolution of the Pilbara Craton and Fortescue Basin. Springer Nature.
Hollister, L.S., 1993. The role of melt in the uplift and exhumation of orogenic belts. Chem. Geol. 108, 31–48.
Hollister, L.S., Crawford, M.L., 1986. Melt-enhanced deformation: a major tectonic process. Geology 14, 558.
Ji, M., Gao, X.-Y., Xia, Q.-X., Zheng, Y.-F., 2024. Secular change of metamorphic features in the Himalayan orogen during the cenozoic and its tectonic implications. Earth-Sci. Rev. 248, 104640.
Jiang, J., Zou, X., Mitchell, R.N., Zhang, Y., Zhao, Y., Yin, Q.-Z., Yang, W., Zhou, X., Wang, H., Spencer, C.J., 2024. Sediment subduction in Hadean revealed by machine learning. Proc. Natl. Acad. Sci. 121, e2405160121.
Johnson, T.E., Kirkland, C.L., Gardiner, N.J., Brown, M., Smithies, R.H., Santosh, M., 2019. Secular change in TTG compositions: implications for the evolution of Archaean geodynamics. Earth. Planet. Sci. Lett. 505, 65–75.
Kröner, A., Hofmann, A., 2019. The Archaean Geology of the Kaapvaal Craton, Southern Africa. Springer.
Lee, C.-T.A., Chin, E.J., 2014. Calculating melting temperatures and pressures of peridotite protoliths: implications for the origin of cratonic mantle. Earth. Planet. Sci. Lett. 403, 273–286.
Macgregor, A., 1951. Some milestones in the Precambrian of Southern Rhodesia. In: Proceedings of the Geological Society of South Africa, pp. 27–71.
Millonig, L., Zeh, A., Gerdes, A., Klemd, R., 2008. Neoarchaean high-grade metamorphism in the Central Zone of the Limpopo Belt (South Africa): combined petrological and geochronological evidence from the Bulai pluton. Lithos 103, 333–351.
Mintrone, M., Galli, A., Schmidt, M., 2022. Exhumation of a migmatitic unit through self-enhanced magmatic weakening enabled by tectonic contact metamorphism (Gruf complex, Central European Alps). Contrib. Mineral. Petrol. 177, 56.
Moyen, J.-F., Martin, H., 2012. Forty years of TTG research. Lithos 148, 312–336.
Nicoli, G., Stevens, G., Moyen, J.F., Frei, D., 2015. Rapid evolution from sediment to anatectic granulite in an archean continental collision zone: the example of the Bandelierkop Formation metapelites, South Marginal Zone, Limpopo Belt, South Africa. J. Metamorph. Geol. 33, 177–202.
O'brien, P., Rötzler, J., 2003. High-pressure granulites: formation, recovery of peak conditions and implications for tectonics. J. Metamorph. Geol. 21, 3–20.
Palin, R.M., Santosh, M., Cao, W., Li, S.-S., Hernández-Uribe, D., Parsons, A., 2020. Secular change and the onset of plate tectonics on Earth. Earth-Sci. Rev. 207, 103172.
Philpotts, A.R., Ague, J.J., 2022. Principles of Igneous and Metamorphic Petrology, 3 ed. Cambridge University Press, Cambridge.
Plank, T., Langmuir, C.H., 1993. Tracing trace elements from sediment input to volcanic output at subduction zones. Nature 362, 739–743.
Poujol, M., Jaguin, J., Moyen, J.-F., Boulvais, P., Paquette, J.-L., 2021. Archaean S-Type granites: petrology, geochemistry and geochronology of the Lekkersmaak and Willie plutons, Kaapvaal Craton, South Africa. S Afr. J. Geol. 124, 87–110.
Reimink, J.R., Smye, A.J., 2024. Subaerial weathering drove stabilization of continents. Nature 629, 609–615.
Roberts, N.M., Yakymchuk, C., Spencer, C.J., Keller, C.B., Tapster, S.R., 2024. Revisiting the discrimination and distribution of S-type granites from zircon trace element composition. Earth. Planet. Sci. Lett. 633, 118638.
Rosenberg, C., Handy, M., 2005. Experimental deformation of partially melted granite revisited: implications for the continental crust. J. Metamorph. Geol. 23, 19–28.
Smye, A.J., Kelemen, P.B., 2025. Ultra-hot origins of stable continents. Nat. Geosci. 18, 1296–1302.
Swanner, E.D., Lambrecht, N., Wittkop, C., Harding, C., Katsev, S., Torgeson, J., Poulton, S.W., 2020. The biogeochemistry of ferruginous lakes and past ferruginous oceans. Earth-Sci. Rev. 211, 103430.
Sylvester, P.J., 1998. Post-collisional strongly peraluminous granites. Lithos 45, 29–44.
Tamblyn, R., Hermann, J., Hasterok, D., Sossi, P., Pettke, T., Chatterjee, S., 2023. Hydrated komatiites as a source of water for TTG formation in the Archean. Earth. Planet. Sci. Lett. 603, 117982.
Tang, M., Chen, K., Rudnick, R.L., 2016. Archean upper crust transition from mafic to felsic marks the onset of plate tectonics. Science 351, 372–375.
Taylor, J., Stevens, G., Buick, I., Lana, C., 2012. Successive midcrustal, high-grade metamorphic events provide insight into mid-archean mountain-building along the SE margin of the proto–Kaapvaal craton. Bulletin 124, 1191–1211.
Thompson, A.B., 1982. Dehydration melting of pelitic rocks and the generation of H 2 O-undersaturated granitic liquids. Am. J. Sci. 282, 1567–1595.
Trail, D., Tailby, N., Wang, Y., Mark Harrison, T., Boehnke, P., 2017. Aluminum in zircon as evidence for peraluminous and metaluminous melts from the Hadean to present. Geochem. Geophys. Geosystems 18, 1580–1593.
Valli, F., Guillot, S., Hattori, K.H., 2004. Source and tectono-metamorphic evolution of mafic and pelitic metasedimentary rocks from the central Quetico metasedimentary belt, Archean Superior Province of Canada. Precambrian. Res. 132, 155–177.
Vanderhaeghe, O., 2009. Migmatites, granites and orogeny: flow modes of partially-molten rocks and magmas associated with melt/solid segregation in orogenic belts. Tectonophysics 477, 119–134.
Wang, D., Guo, J., 2017. Late Archean high-pressure pelitic granulites in the Yinshan block, North China Craton. Precambrian. Res. 303, 251–267.
Wang, X., Tang, M., Moyen, J., Wang, D., Kröner, A., Hawkesworth, C., Xia, X., Xie, H., Anhaeusser, C., Hofmann, A., 2022. The onset of deep recycling of supracrustal materials at the Paleo-Mesoarchean boundary. Natl. Sci. Rev. 9, nwab136.
White, R., Powell, R., Holland, T., 2007. Progress relating to calculation of partial melting equilibria for metapelites. J. Metamorph. Geol. 25, 511–527.
D.L. Whitney, C. Teyssier, A.K. Fayon, 2004. Isothermal decompression, partial melting and exhumation of deep continental crust.
Yu, C., Yang, T., Zhang, J., Zhao, G., Cawood, P.A., Yin, C., Qian, J., Gao, P., Zhao, C., 2022. Coexisting diverse P–T–t paths during neoarchean Sagduction: insights from numerical modeling and applications to the eastern North China Craton. Earth. Planet. Sci. Lett. 586, 117529.
Zhao, G., Zhai, M., 2013. Lithotectonic elements of precambrian basement in the North China Craton: review and tectonic implications. Gondwana Res. 23, 1207–1240.
Zhu, Z., Campbell, I.H., Allen, C.M., Burnham, A.D., 2020. S-type granites: their origin and distribution through time as determined from detrital zircons. Earth. Planet. Sci. Lett. 536, 116140.